Construction and Building Materials 392 (2023) 131976

Contents lists available at ScienceDirect

Construction and Building Materials

journal homepage: www.elsevier.com/locate/conbuildmat

Long-term properties of self-cleaning alkali-activated slag-based mortars with titanium dioxide nanoparticles

D. Coffetti [a,b,*], E. Crotti [a], L. Coppola [a,b]

[a] Department of Engineering and Applied Sciences, University of Bergamo, Viale Marconi, 5, 24044 Dalmine, BG, Italy
[b] National Interuniversity Consortium of Materials Science and Technology (INSTM), Research Unit of Bergamo, 50121 Florence, Italy

ARTICLE INFO

Keywords:
Alkali activated materials
Photocalitic mortar
TiO_2 nanoparticles
Accelerated tests
Outdoor natural exposure

ABSTRACT

Titanium dioxide (TiO_2) is considered one of the most efficient photocatalysis to produce self-cleaning cementitious materials. At the same time, alkali activated binders have become one of the most interesting low-carbon alternatives to Portland cement. For this, the addition of titanium dioxide nanoparticles in one-part alkali-activated slag-based (AAS) mortars was analyzed to evaluate the effect on the rheological and mechanical properties, dirt pick-up resistance as well as self-cleaning capability. This paper reports a two-year campaign of outdoor exposure in an industrial environment in Northern Italy to investigate the natural photoactivity of the mortars doped with different TiO_2 dosages. The experimental results indicated limited effect of nanoparticles on the rheology and mechanical properties of AAS mortars. It was also highlighted the beneficial effect of TiO_2 addition in self-cleaning capability under natural and accelerated conditions and the fundamental role in photocatalytic efficiency of the alkali content.

1. Introduction

The interest in the photocatalytic properties of cementitious materials has grown enormously in the last decades by both academic researchers and construction companies. Since the first studies of Fujishima and Honda [1,2], the capability of nano-titanium dioxide (TiO_2) to promote the self-cleaning of materials and to reduce pollutants such as volatile organic compounds (VOCs) and nitrogen oxides (NOx) under artificial light irradiation (UV light) or sunlight was evident. The process of photodecomposition through light absorption of TiO_2 is considered one of the most powerful photocatalysis actually available and could be advantageously used, in combination with cementitious materials, on a large-scale to improve the performances of buildings and civil structures [3].

In the last years, the use of titanium dioxide in construction materials have been widely investigated to obtain "smart" concretes, mortars, plasters and coatings for self-cleaning roads, facades, tunnel linings and internal walls with added antipollution ability [4–8]. "Smart" concrete pavements and external building envelopes benefit from their flat configuration which promotes the insolation allowing to reduce the urban air pollution level, maintain their aesthetic aspect and conserve the solar reflectance and thermal emittance which can be jeopardized by the combined action of soiling and weathering, thus increasing the energy requirement of cities [9–11]. Internal plasters doped with TiO_2 nanoparticles could be capable of preventing the accumulation of VOCs released by cleaning agents, cigarette smoke, adhesives and paints even with limited UV light due to the usually limited concentration of VOCs in indoor environments [12,13]. Finally, one of the most promising applications of photocatalytic cementitious materials is in road tunnels characterized by a relatively closed and poorly ventilated environment which makes the exhaust car emissions removal challenging, thus determining harm to human health, reducing visibility and hindering the traffic safety [14,15]. Therefore, the use of self-cleaning materials for tunnel lining combined to a proper artificial lighting system could improve the traffic safety and environmental hygiene of tunnels and reduce the periodic maintenance cost mainly related to the cleaning procedure that requires the infrastructure to be closed to traffic with inconvenience to users.

During the last years, several studies have been conducted on the properties of cement-based materials containing titanium dioxide nanoparticles, especially on the influence of the nano-addition on the mechanical, photocatalytic and self-cleaning properties of mixtures [16–18]. Moreover, the durability of these systems has been investigated by means of natural exposure tests and accelerated laboratory

* Corresponding author.
E-mail address: denny.coffetti@unibg.it (D. Coffetti).

https://doi.org/10.1016/j.conbuildmat.2023.131976
Received 20 March 2023; Received in revised form 1 May 2023; Accepted 26 May 2023
Available online 3 June 2023

procedures [19,20]. On the contrary, the knowledge on the use of TiO_2 in alkali-activated slag-based binders (AAS), one of the most promising "green" alternatives to Portland cement [21–23], is very limited and it refers only to the so-called "two-part" AAS. To date, only very few papers dealing with the influence of titanium dioxide on the properties of AAS mixtures [24–27]. First of all, it was highlighted that the addition to TiO_2 enhances the hydration process of slag and promote a denser microstructure thus improving the mechanical properties of AAS mixtures from 5% to 15% depending on the dosage and the physical properties of the nanoparticles [24,27]. Yang et al. [27] and El-Kattan et al. [25] investigated also the volumetric stability of these systems, evidencing a reduction in shrinkage due to the formation of novel expansive products such as titanium silicate hydrate (T-S-H) and C_4TiH_{13}. Only Llano-Guerrero et al. [24] evaluated the self-cleaning capability of TiO_2-doped AAS pastes by means of accelerated tests with rhodamine B, showing low photocatalytic activity in comparison with metakaolin-based geopolymers.

Following from the limited knowledge in this field, the addition of titanium dioxide nanoparticles in one-part alkali-activated slag-based mortars was analyzed to evaluate the effect on the rheological and mechanical properties, dirt pick-up resistance as well as self-cleaning capability. In addition, this paper reports a two-year campaign of outdoor exposure in an industrial environment in Northern Italy to investigate the natural photoactivity of the mortars doped with different TiO_2 dosages.

2. Materials

Twelve alkali activated mortars were manufactured with a highly amorphous (Fig. 1) ground granulated blast furnace slag (GGBFS) with 28-day pozzolanic activity index K = 0.76 (according to EN 196–5), basicity coefficient Kb = 1.20 and quality coefficient Kq = 1.77, according to Wang et al. [28]. The Kb and Kq coefficients were determined with the Eq. (1) and Eq. (2).

$$Kb = \frac{CaO + MgO}{SiO_2 + Al_2O_3} = 1.20 \quad (1)$$

$$Kq = \frac{CaO + MgO + Al_2O_3}{SiO_2 + TiO_2} = 1.77 \quad (2)$$

An alkaline powder blend previously developed by the authors (laboratory grade sodium metasilicate pentahydrate, potassium hydroxide and sodium carbonate with relative mass ratio of 7:3:1) was also used as solid activator [29]. Moreover, eight Portland cement-based mortars were manufactured as reference by using a grey Portland cement CEM I 52.5R and a white Portland cement CEM I 52.5R. Table 1 reports the main physical properties and the chemical composition of binders, evaluated by means of laser granulometry (Mastersizer 3000 Malvern Instruments Ltd, Malvern. UK) and SEM-EDS measurements (Inspect. FEI Company. Hillsboro. OR. USA), respectively.

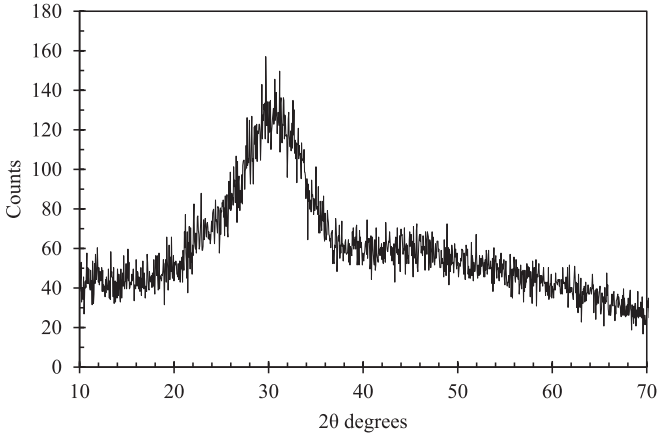

Fig. 1. XRD pattern of GGBFS (Rigaku Miniflex 60, X-ray source Cu K-alpha 0.15418 nm, 40 kV. 15 mA, theta step 0.02, rate 1°/min).

Five different natural siliceous sands having maximum size of 2.5 mm were combined as fine aggregates. Furthermore, a commercial polycarboxylate-based superplasticizer was used to ensure a plastic consistency of cementitious mortars.

Nano-sized TiO_2 with a specific mass of 4.2 kg/dm^3 was used in the current study to obtain mortars with photocatalytic properties and engage self-cleaning capability of alkali activated slag-based materials. The main properties of the nanoparticles are reported in Table 2.

3. Mixtures, preparation and sample curing

Three different type of one-part AAS mortars were produced by varying the activator/precursor ratio between 8 and 16. In addition, cementitious mortars manufactured with Portland cement (grey or white cement) were used as control mix. In all mixtures, the water-to-binder ratio was set at 0.55 and the sand-to-binder ratio was fixed at 3.0 while different amounts of TiO_2, i.e. 0%, 1%, 3% and 5% with respect to the binder mass, were used to evaluate the impact of titanium dioxide dosage on rheological properties, compressive strength, dynamic elastic modulus, self-cleaning ability (both under natural and accelerated conditions) and resistance to fouling of AAS materials. The dosages of the titanium dioxide in powder form were selected starting from the research by Diamanti et al. [5] on the photocatalytic and superhydrophilic properties of cementitious mortars containing TiO_2. The composition of the mortars is reported in Table 3 (WC: White cement-based mortars; GC: grey cement-based mortars; S: Alkali-activated slag-based mortars. The number indicates the activator-to-slag ratio by mass; the number after the hyphen indicates the TiO_2 dosage).

Superplasticizer (when used) was first mixed with water by means of a high shear mixer for 3 min at 250 rpm, then mortars were prepared by blending binders, solid activators (if present), sand, nano-size TiO_2 in powder form and mixing water by using an automatic mortar mixer compliant with EN 196–1. The fresh mortars were portioned into 4 parts: the first part was used to carry out the fresh state tests, the second to manufacture 40x40x160 mm^3 prisms for the elasto-mechanical tests, the third to produce 80x100x10 mm^3 tiles for the accelerated photocatalytic, dirt pick up resistance tests and bulk and surface analysis while the last was applied with a thickness of 10 mm on bricks for self-cleaning evaluations under natural conditions. All the samples were finished by using a steel float in order to achieve a smooth surface and they were kept in a climatic chamber (20 °C, 95% R.H.) for 24 h before demolding (Table 4). After this, the specimens were cured in the same conditions until tests.

4. Experimental setup

4.1. Fresh and elasto-mechanical properties

The workability, the specific mass at fresh state and the air content were detected in accordance with EN 1015-3, EN 1015-6 and 1015-7, respectively. Moreover, the setting time was determined by using Vicat's apparatus in accordance with EN 196-1. Compressive strength was determined at 1, 7 and 28 days from casting (EN 1015-11). Finally, dynamic modulus of elasticity of mixtures was estimated by means of Ultrasonic Digital Indicator Tester at 1, 7 and 28 days in accordance with EN 12504-4.

4.2. Bulk and surface characterization

The structure of all cementitious and alkali-activated mortars was characterized at micro- and macroscopic level in terms of surface roughness and TiO_2 nanoparticles distribution. Surface roughness was

Table 1
Chemical composition and physical properties of binders.

Component wt.%	CaO	Al_2O_3	SiO_2	Fe_2O_3	SO_3	TiO_2	K_2O	MgO	Others	Spec. Mass [kg/dm^3]	Spec. surface [m^2/kg]
Grey cement	63.7	5.2	19.1	3.5	2.9	0.3	0.6	1.1	3.6	3.0	350
White cement	68.3	2.4	21.7	0.9	2.1	0.5	0.4	0.9	2.8	3.0	360
GGBFS	45.8	10.0	32.8	1.5	0.2	2.0	0.5	6.4	0.8	3.1	345

Table 2
Main properties of nano-sized TiO_2 (provided by the supplier).

Property	Value
Specific surface	7 – 9 m^2/g
Mean particle size	250 nm
Phisical form	White powder
Loss on drying (2 h – 105 °C)	1.0%
Crystal modification	Anatase (80%) – Rutile (20%)
TiO_2 content	> 99%
Al_2O_3 content	< 0.3%
SiO_2 content	< 0.2%
Fe_2O_3 content	< 0.1%
HCl content	< 0.3%

determined by means of a focus detection system based on the dynamic focusing principle of the confocal microscope Keyence VHX-7100 that works on the detection of the focus position of reflected light from the surface, allowing to determine the heigh value. For all samples the assessment of the surface roughness is based on the S_a parameter that expresses the difference in height of each point compared to the arithmetical mean of the surface. The cutoff wavelength for S- and L-filter were fixed at 100 μm and 10 mm, respectively.

Moreover, in order to evaluate the TiO_2 nanoparticles distribution inside the samples, scanning electron microscope (SEM) observations and X-ray spectroscopy (EDS) analyses have been carried out using a Zeiss EVO 50 equipped with an Oxford x-act probe for energy-dispersive X-ray spectroscopy both on the fracture surfaces (bulk material) and on the external surface finished with steel float.

4.3. Accelerated photocatalytic tests

Self-cleaning capability of TiO_2-containing mortars was determined by monitoring the discoloration of organic dyes (rhodamine B (RhB) and methylene blue (MB)) according to the procedure reported in the Italian standard UNI 11259. The solutions of organic dyes were prepared by stirring for 5 min at 500 rpm 1 g of rhodamine B or the methylene blue in 1 L of distilled water. Subsequently, a hydrophobic product was applied on the 28-days old mortar tiles to delimit an area of 22 cm^2 to be tested. After complete drying of the hydrophobic agent, 0.5 ml of aqueous solution was carefully sprayed onto the test surface and then left to dry in a dark room at 20 °C, 60% R.H for 24 h. Finally, the samples were exposed to a UV-A source with irradiance equal to 3.75 ± 0.25 W/m^2. The color variation was determined after 4 and 24 h of exposure to UV light by measuring the a* coordinate (redness/greenness for RhB) or b* coordinate (yellowness/blueness for MB) by means of a portable spectrophotometer (PCE-CSM 4, PCE Instruments Italia) working on CIELAB color space. The following equations (Eq.3 and Eq.4) were used to evaluate the color variations:

$$a_{\%} = \frac{a_0^* - a_t^*}{a_0^*} \bullet 100 \quad (3)$$

Table 4
Geometrical properties and numerousness of hardened samples used during the research.

Test	Ages of sample	Sample format	Sample size	Number of samples by mortar type
Compressive strength	1–7-28 days	Prisms	40x40x160 mm^3	9 (3 for each age)
Bulk and surface characterization	28 days	Tiles	80x100x10 mm^3	5
Accelerated photocatalytic tests	28 days	Tiles	80x100x10 mm^3	5
Dirt pick-up resistance	28 days	Tiles	80x100x10 mm^3	5
Outdoor natural photocatalytic tests	28 days	Brick with mortar	Thickness 10 mm	4

Table 3
Detailed mix proportions of mortars.

	White cement	Grey cement	GGBFS	Sand	Water	Activators [% vs binder]	Superplasticizer [% vs binder]	TiO_2 [% vs binder]
WC-0	1			3	0.55		0.5%	0%
WC-1	1			3	0.55		0.5%	1%
WC-3	1			3	0.55		0.5%	3%
WC-5	1			3	0.55		0.5%	5%
GC-0		1		3	0.55		0.5%	0%
GC-1		1		3	0.55		0.5%	1%
GC-3		1		3	0.55		0.5%	3%
GC-5		1		3	0.55		0.5%	5%
S8-0			1	3	0.55	8%		0%
S8-1			1	3	0.55	8%		1%
S8-3			1	3	0.55	8%		3%
S8-5			1	3	0.55	8%		5%
S12-0			1	3	0.55	12%		0%
S12-1			1	3	0.55	12%		1%
S12-3			1	3	0.55	12%		3%
S12-5			1	3	0.55	12%		5%
S16-0			1	3	0.55	16%		0%
S16-1			1	3	0.55	16%		1%
S16-3			1	3	0.55	16%		3%
S16-5			1	3	0.55	16%		5%

$$b_{\%} = \frac{b_0^* - b_t^*}{b_0^*} \bullet 100 \quad (4)$$

where a_0^* and b_0^* are the color intensity coordinates of specimens before the UV irradiation, a_t^* and b_t^* are the color intensity coordinates of specimens at t hours of irradiation.

4.4. Dirt pick-up resistance

The tendency of the different mixtures to absorb and retain dust and other impurities deposited on the surface was observed in accordance with Italian standard UNI 10792. In particular, five 80x100x10 mm^3 mortar samples were partially immersed for 30 s in a black solution (1% of hydro-dispersible carbon black paste in distilled water), then the specimens were washed in tap water for about 10 s, dried with an absorbent cloth and left to dry for 24 h at a room temperature (20 °C ± 2 °C). After 24 h, the difference in lightness (ΔL) between the part of specimens that was immersed and the part that was not immersed was measured by using a portable spectrophotometer. Furthermore, the black solution absorption of the mortars was also determined by weighting the sample.

4.5. Outdoor natural photocatalytic tests

Forty different samples of mortars applied on bricks were exposed to the polluted industrial environment of the Po Valley (Northern Italy) for 2 years. Specimens were put on tilted supports (45° with respect to the ground) on the rooftop of the Engineering Laboratory of the University of Bergamo in order to ensure homogeneous exposure to sunlight without shading and to avoid stagnating rain water on mortar surfaces. One half of mortar samples were positioned facing South while the other half was facing North in order to evaluate the influence of the different exposure on the self-cleaning capability of alkali activated materials. Specimens were monitored over time by measuring the color variation on CIELAB color space ΔE, corresponding respectively to the color at the time t and to the initial color at t = 0, by means of the Eq. (5):

$$\Delta E = \sqrt{\left(L_t^* - L_0^*\right)^2 + \left(a_t^* - a_0^*\right)^2 + \left(b_t^* - b_0^*\right)^2} \quad (5)$$

With L_t^*, a_t^* and b_t^* chromatic coordinates at time t and L_0^*, a_0^* and b_0^* chromatic coordinates before the exposure to the polluted urban environment. The measurements were done after a rainy day in order to test samples without detached atmospheric soling that would cause a gray shift of the color and thus unreliable results.

5. Results and discussion

5.1. Fresh state properties

Fig. 2 shows the flowability of fresh mortars as a function of titanium dioxide content. Even if other authors evidenced the key modification induced by TiO_2 nanopowders in fresh cementitious mixtures is a decrease in workability, all the samples (both cementitious and alkali activated) show a consistency in the range of 150–200 mm of spreading on the flowing table without significant variations as the TiO_2 nanoparticles dosage increases. This could be explained with the higher average size of titanium dioxide nanoparticles with respect to those used by Meng et al. [30] and Suneel et al. [31]. Moreover, as expected, the increase in alkali content leads to an increase in the workability of the mixtures. This behavior is caused by the deflocculating and plasticizing effect promoted by the use of sodium silicate as activator that reduce the yield stress at early ages [32].

The air content and the specific mass at fresh state of mortars containing nano-TiO_2 are similar, regardless of the nanoparticles content (Table 5). The cementitious mortars are characterized by an entrapped air volume close to 6% while alkali-activated slag-based mixtures are in the range of 3.5–5.2%. Similarly, the variation of specific mass of fresh mortars due to the use of nanoparticles is negligible (lower than 1.5%).

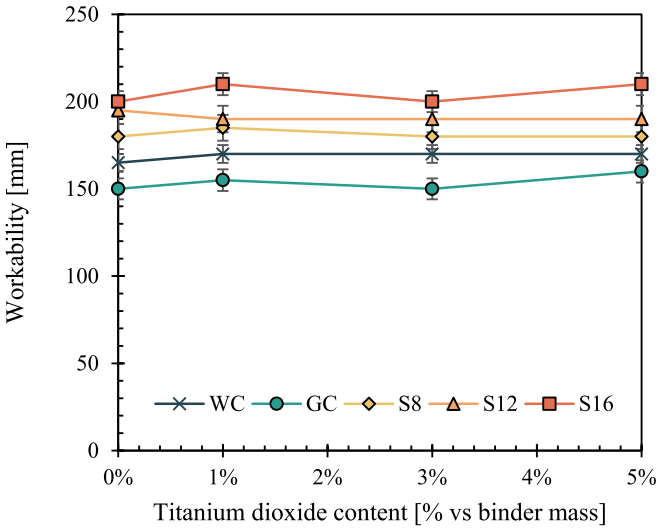

Fig. 2. Flowability of fresh mortars as a function of TiO2 content.

Table 5
Air content and specific mass at fresh state of mortars.

	TiO_2 content [% vs binder mass]			
	0%	1%	3%	5%
GC	6.0% (2120)	6.0% (2130)	5.5% (2150)	5.5% (2145)
WC	6.4% (2165)	6.0% (2165)	6.3% (2185)	5.8% (2165)
S8	5.2% (2120)	4.6% (2135)	5.2% (2125)	5.2% (2140)
S12	4.9% (2145)	5.2% (2140)	5.1% (2165)	5.0% (2155)
S16	4.0% (2175)	3.5% (2190)	3.8% (2180)	4.6% (2190)

On the contrary, the addition of titanium dioxide affects the setting time of fresh mixtures as reported in Fig. 3. The initial setting time of cementitious and alkali-activated mortars decreases with the increase of the nanoparticles content up to about 60 min while the opening time remains constant by varying the dosage of nano-TiO_2. Only the alkali-activated S8 evidences a decrease in opening time when nanopowders are added to the mixture. This behavior has already been highlighted by Zhang et al. [33] in cement-based mortars due to a seeding effect promoted by nanoparticles.

5.2. Elasto-mechanical performances

Table 6 shows the elasto-mechanical properties of mortars manufactured with different amount of TiO_2 nanoparticles. The 28-day compressive strength of plain WC, GC and S16 are similar and they are in the range of 41–44 MPa while alkali-activated mixtures with lower activators content (S8 and S12) evidence compressive strength after 28 days equals to 16.0 and 23.8 MPa, respectively. On the contrary, at early ages (1 day), the compressive strength of cementitious mixes is higher with respect to that of alkali-activated ones. The dynamic modulus of elasticity (DME) is influenced by both the nature of the binder and the compressive strength of mortars. Cementitious mixtures without nanoparticles exhibits DMEs close to 26–27 GPa at 1 day and 35–36 GPa at 28 days while alkali-activated S16 mortar, even if has a compressive strength similar to that of WC and GC, evidences slightly lower values both at early (24 GPa) and late (31 GPa) ages. Finally, S8 and S12 are characterized by DMEs equal to 26 and 30 GPa, respectively.

The addition of titanium dioxide nanoparticles seems to have only a marginal effect on the elasto-mechanical properties of mortars at early ages. On the contrary, the 28-day compressive strength of cementitious mixtures linearly increases with the addition of nanoparticles (Fig. 4),

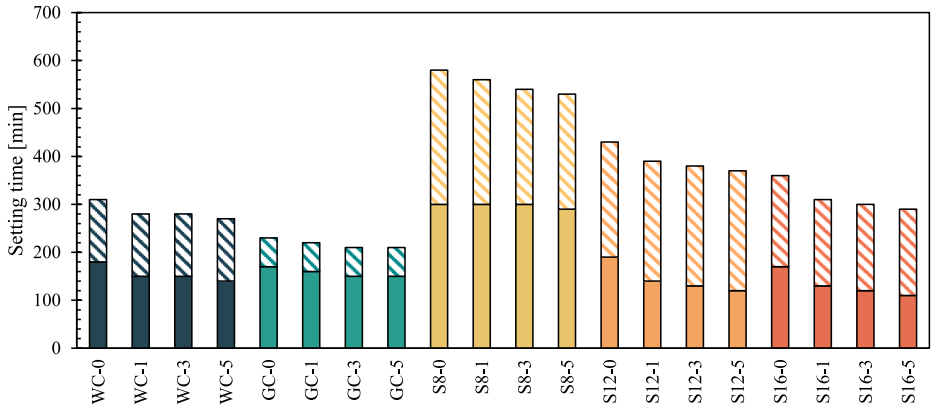

Fig. 3. Initial (solid color fill) e final (pattern fill) setting time of mortars.

Table 6
Elasto-mechanical properties of mortars.

	Compressive strength [MPa]			Elastic modulus [GPa]		
	1d	7d	28d	1d	7d	28d
WC-0	18.2	35.1	41.2	25.3	33.3	35.2
WC-1	17.1	36.4	41.6	25.8	34.0	35.3
WC-3	18.7	39.3	45.2	25.7	33.6	35.3
WC-5	19.3	41.3	45.3	25.8	34.0	35.1
GC-0	25.0	42.1	44.8	26.4	35.6	36.5
GC-1	25.7	40.8	45.7	26.2	35.4	36.1
GC-3	26.0	44.0	48.1	26.8	35.4	35.7
GC-5	26.8	44.3	49.5	27.0	36.0	36.1
S8-0	5.1	16.0	22.9	16.8	24.1	25.9
S8-1	5.8	17.9	25.8	18.9	25.8	27.7
S8-3	5.9	18.8	26.0	18.3	26.0	27.6
S8-5	5.6	18.1	25.0	17.6	26.0	28.1
S12-0	10.1	23.8	36.4	23.0	27.8	29.9
S12-1	10.1	24.1	37.1	23.1	27.8	30.2
S12-3	10.0	24.6	36.5	23.1	28.0	30.6
S12-5	10.5	24.9	36.4	23.4	28.1	30.8
S16-0	14.2	31.3	43.4	24.8	28.9	31.3
S16-1	14.0	30.1	44.0	24.6	28.8	31.7
S16-3	15.8	30.4	44.8	24.7	28.9	31.9
S16-5	16.1	31.7	43.7	25.1	28.9	31.6

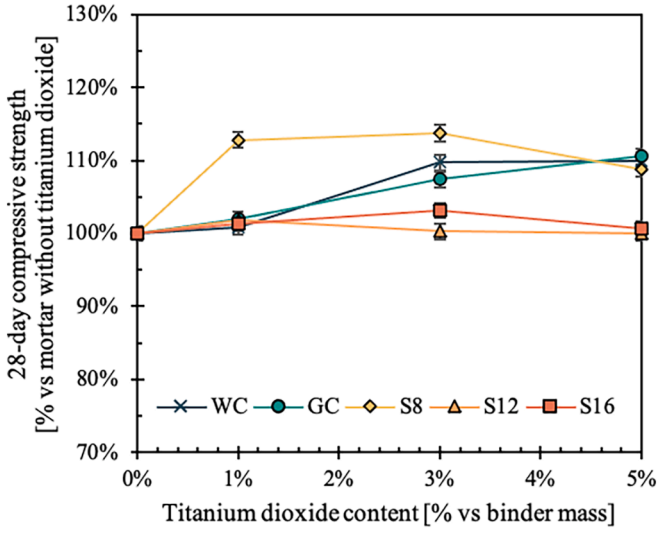

Fig. 4. 28-day compressive strength of mortars as a function of TiO_2 content.

up to + 10% when 5% of TiO_2 nanoparticles with respect to binder mass is used. This behavior was also highlighted by Shafaei et al. [34] that attributed it to the micro-filling effect of the fine titanium dioxide which promotes the formation of denser microstructures, improving the strength of cementitious mixtures, while Chen et al. [4] confirmed that nano-TiO_2 is a non-reactive fine filler without pozzolanic activity, acting as potential nucleation sites for the accumulation of hydration products. On the contrary, alkali activated-based mortars do not evidence significant improvements in 28-day compressive strength when titanium dioxide nanoparticles were added to the mixtures, with the exception of the TiO_2-containing S8 mortar which evidences an increase in strength from 9 to 14% with respect to the S8 mortar manufactured without nano-TiO_2.

5.3. *TiO_2 nanoparticles distribution*

In order to evaluate the TiO_2 nanoparticles distribution inside the binder matrix, SEM observations and EDS analyses have been carried out both on the fracture surfaces (bulk material) and on the external surface finished with steel float. EDS maps confirmed that the TiO_2 nanoparticles are homogeneously distributed in the cementitious and alkali-activated matrix with no significant differences between bulk and external surfaces (Fig. 5).

5.4. *Accelerated photocatalytic tests*

Fig. 6 reports the color variation a% of mortars sprayed with rhodamine B after 4 and 24 h of exposure to UV light as a function of titanium dioxide nanoparticles content. The cementitious mortars WC and GC manufactured without TiO_2 exhibit a moderate self-cleaning capability as already evidenced by Tyukavkina et al. [35] and Shen et al. [36] with a color variation a% equals to 5% and 16% for WC and 8% and 26% for GC after 4 and 24 h, respectively. On the contrary, the color variation a% of TiO_2-free alkali-activated slag-based mortars is less than that shown by cementitious mortars, regardless of the alkali content (S8, S12 or S16) and the exposure time to UV light.

The beneficial effect of TiO_2 addition in self-cleaning capability is evident both in cementitious and alkali-activated mortars. In particular, regardless of UV light exposure time, the color variation a% increases almost linearly by increasing the nanoparticles content, with the exception of the GC mortar which appears to be little affected by the titanium dioxide dosage. Similar results can be found in Fig. 7 where the color variation b% of mortars treated with methylene blue after different UV light exposure was plotted as a function of TiO_2 content. In general, it can be noted that the ability of UV light to discolor MB is higher to that with RhB, regardless of the composition of cementitious or alkali-activated mortars.

In order to evaluate the efficiency of the TiO_2 nanoparticles addition

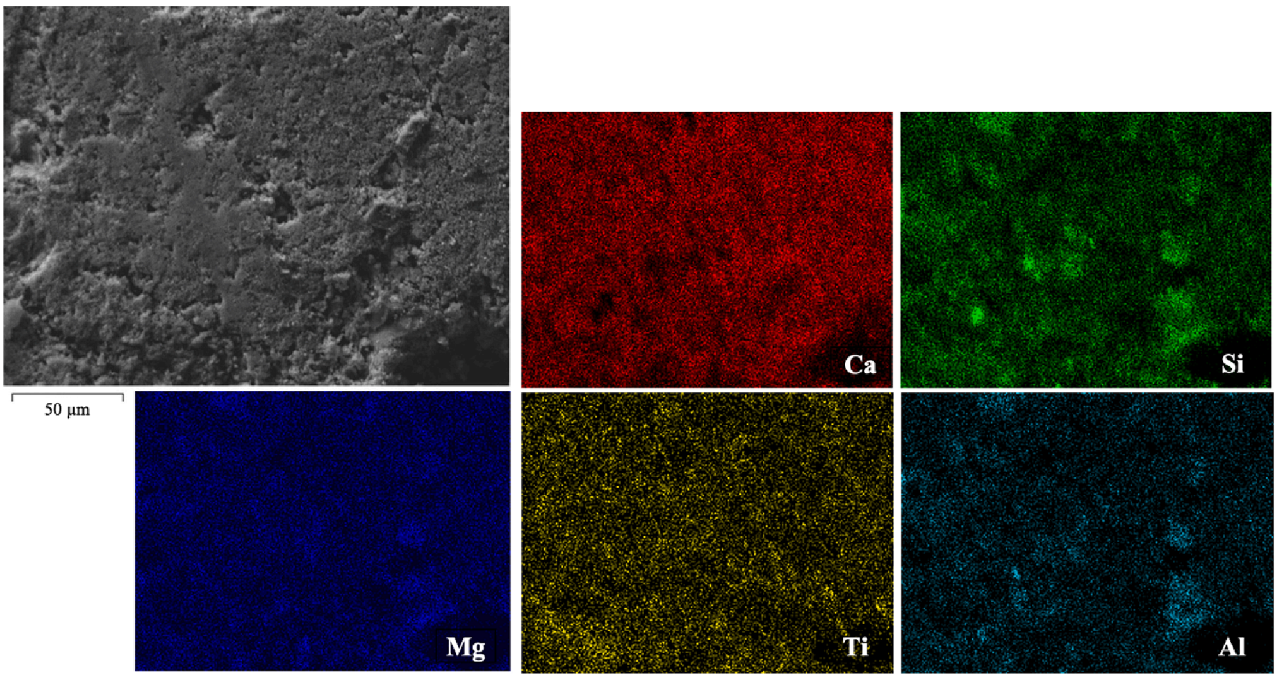

Fig. 5. SEM observation and EDX analysis of the external surface of S12-5 sample.

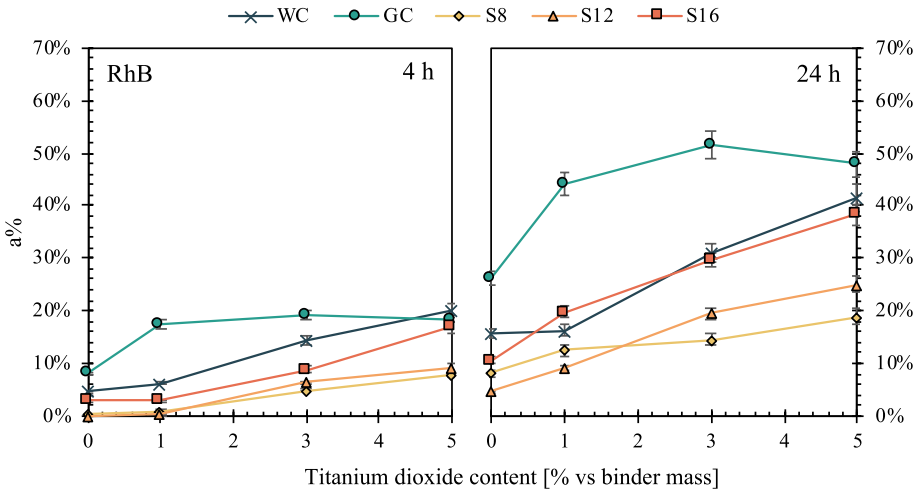

Fig. 6. A% variations as a function of titanium dioxide content after 4 h (left) and 24 h (right).

on mortars with different intrinsic ability to degrade organic dyes, the dimensionless efficiency coefficient Γ was calculated as the average slope of the curves a% and b% vs TiO_2 content (with the exception of the GC samples which showed a non-linear trend in Figs. 6 and 7). Results reported in Table 7 evidence that the alkali content in AAS mortars plays a fundamental role in the efficiency of the titanium dioxide nanoparticles to promote the self-cleaning capability, regardless of dyes sprayed on the surface of samples. In fact, when RhB is applied on samples the Γ_{24h} coefficient is 0.0195 for S8, 0.0418 for S12 and 0.0536 for S16 while the cementitious based WC mortar evidenced an efficiency coefficient of 0.0552. Similarly, the Γ_{24h} coefficient of specimens sprayed with MB is influenced by the alkali content of AAS even if the differences between S8, S12 and S16 are smaller than those evidenced by the AAS samples tested with RhB. The samples GC are not included in Table 7 because there is not a linear relationship between a% (RhB) or b % (MB) and TiO_2 content as reported in Figs. 6 and 7.

The different self-cleaning behavior of mortars could be ascribed not only to the nature of the binder but also to the different roughness of the samples (Table 8) evaluated through the Sa (arithmetic mean height) parameter. In fact, regardless of the TiO_2 content, the average Sa parameter for cementitious mixtures is close to 41.8 and 36.2 µm for WC and GC samples, respectively. On the contrary, this parameter is higher for AAS mortars and it is equal to 44.8 (S16), 48.5 (S12) and 55.5 µm (S8). In general, the lower the roughness of the samples, the higher the efficiency coefficient Γ.

Finally, it can be noted in Fig. 8 that the efficiency of degradation is strongly influenced by the chemical nature of dyes. In fact, in accordance with findings reported by Zhu et al. [37], composites containing TiO_2 are more efficient to discolor MB with respect to RhB under UV light due to the different HOMO (Highest Occupied Molecular Orbital) energy gap of RhB (-10.128 eV) and MB (-10.494 eV) which affect the ease of electron transfer in photocatalysis.

5.5. *Dirt pick-up resistance*

Fig. 9 reports the brightness loss (ΔL) as a consequence of the

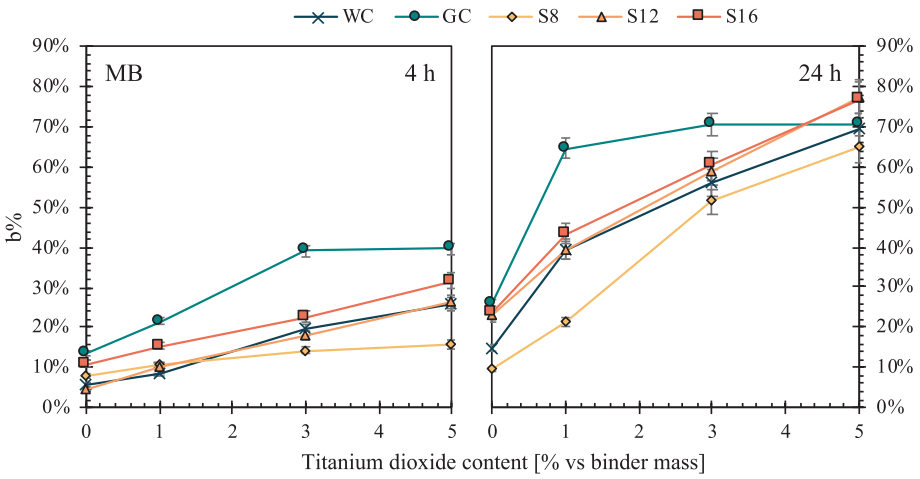

Fig. 7. B% variations as a function of titanium dioxide content after 4 h (left) and 24 h (right).

Table 7
Efficiency coefficient Γ of mortars.

	RhB		MB	
	4 h	24 h	4 h	24 h
WC	0.0325	0.0552	0.0425	0.1021
S8	0.0156	0.0195	0.0154	0.1012
S12	0.0201	0.0418	0.0405	0.1055
S16	0.0289	0.0536	0.0442	0.1148

Table 8
Roughness parameter Sa [μm] of different mortars.

	TiO_2 content				Average
	0%	1%	3%	5%	
WC	42.3	41.7	39.7	43.6	41.8
GC	36.2	35.9	36.0	36.6	36.2
S8	56.0	56.2	55.5	54.2	55.5
S12	47.9	48.2	49.0	48.9	48.5
S16	44.7	44.6	44.2	45.9	44.8

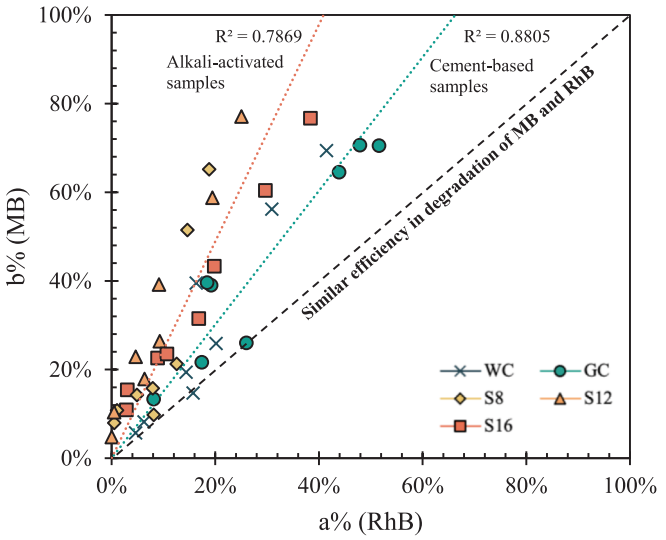

Fig. 8. Color variation under UV light of mortars treated with RhB (a%) and MB (b%). Linear correlation in orange for AAS materials, in green for cementitious mortars. (For interpretation of the references to color in this figure legend, the reader is referred to the web version of this article.)

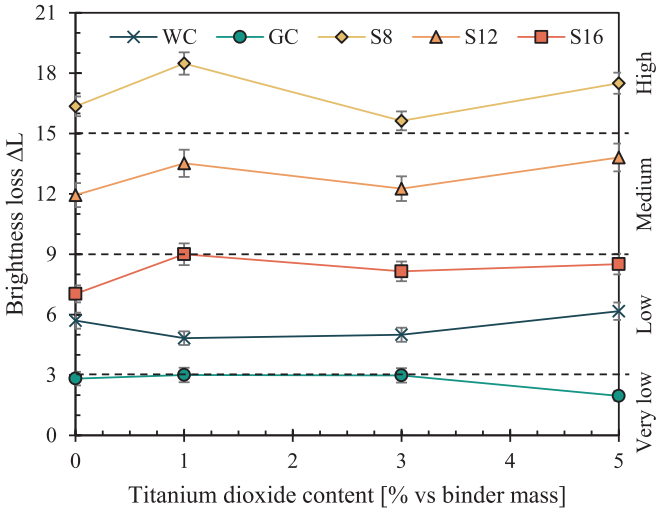

Fig. 9. Brightness loss (ΔL) as a consequence of immersion in carbon black solution for different mortars containing TiO_2. On the right axes the limits identified by the standard UNI 10792 are reported.

immersion of mortars in carbon black solution to investigate the tendency of samples to retain ultra-fine particles; the higher the brightness loss, the lower the dirt pick-up resistance. It can be noted that the resistance to dirtiness of mortars is not influenced by the addition of titanium dioxide but differs by varying the binder nature (cementitious mortars WC and GC are less susceptible to dirt pick-up with respect to alkali-activated mixtures) and the alkali content (the higher the activator dosage, the lower the brightness loss). In particular, after the exposure to carbon black-based solution, the brightness loss was very low for GC, low for WC and S16, medium for S12 and high for S8 in accordance with the limits reported in the Italian standard UNI 10792.

This behavior is primarily attributable to the different roughness of mortars but also to the very different porosity of the outermost layer of the mixtures, investigated by evaluating the absorption of solution containing carbon black. Fig. 10 reports the brightness loss as a function of the carbon black-based solution absorption and it shows that the porosity of the external layers is very different among the AAS mortars; the higher the alkali content, the lower the porosity and thus the higher the dirt pick-up resistance (ΔL). At the same time, it is also evident the effect of the surface properties of samples (i.e., superficial roughness) on the brightness loss of samples after immersion in carbon black-based solution (Fig. 11). As expected, smooth surfaces are less prone to

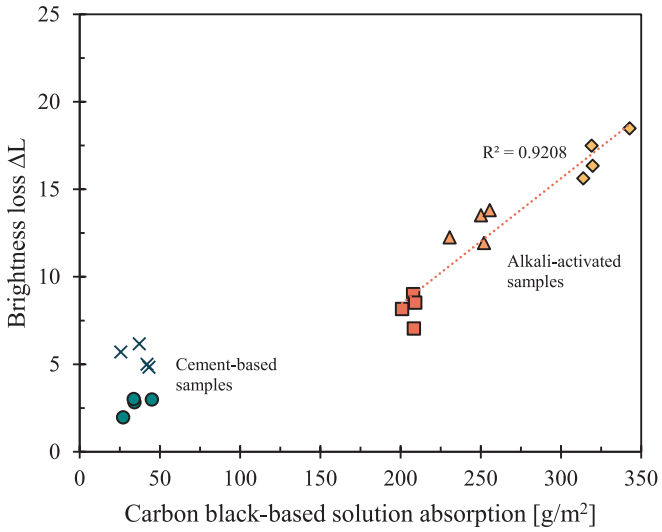

Fig. 10. Brightness loss as a function of the absorption of carbon black-based solution during the dirt pick-up resistance test. The immersion time of samples was 30 s.

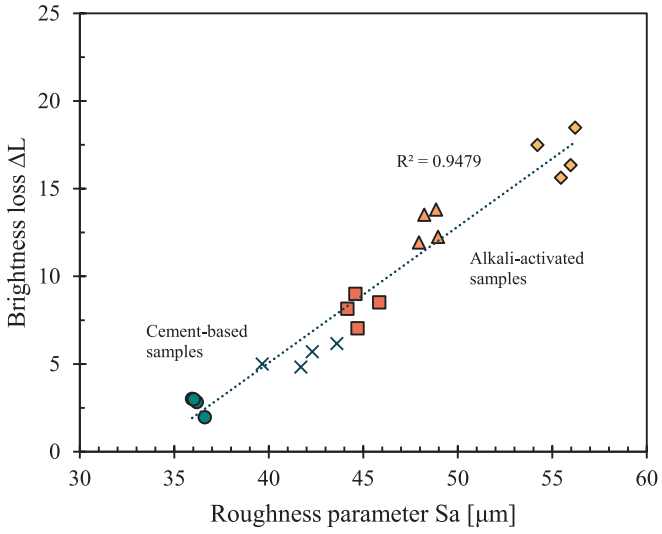

Fig. 11. Brightness loss as a function of the superficial roughness evaluated through Sa parameter.

surface soiling than rough ones, regardless of the titanium dioxide content, due to the greater ease of dirt particles to settle permanently in the valleys of the surface.

5.6. Outdoor natural exposure

The self-cleaning ability, induced by titanium dioxide, has been evaluated by measuring the color variation during the exposure of mortar samples to the polluted industrial environment for 2 years where the rainfall ranging from 0 to 50 mm/hour and global radiation reaches maximum values close to 1000 W/m^2 (Fig. 12). First of all, it can be noted that, before exposure to the polluted environment, the chromatic differences in mortar samples depend almost exclusively on the binder type (white cement, grey cement or alkali-activated slag) used. In fact, the addition of TiO_2 determines only marginal variations in the L* parameter which are reflected in visually not appreciable color changes (Table 9).

The color variation ΔE of samples exposed to the external environment mainly occurred in the first 90 days, beyond which only limited changes were observed to the L*, a* and b* coordinates, regardless of the TiO_2 content added to the material. This trend over time, common to all the mortars investigated, is shown in Fig. 12 which displays the ΔE value over time for the alkali-activated S12 mortars exposed to the South.

After 2 years of exposure (Fig. 13), it can be seen that the color variation of reference samples (without TiO_2) is strongly influenced by the binder type and, only for AAS systems, alkali content. Regardless of the orientation (North or South), grey cement-based mortars GC show ΔE close to 6 while WC and high alkali content AAS (AAS 12 and AAS16) evidence ΔE in the range of 7.5–8.5. Similarly to the dirt pick-up resistance, also the exposure to polluted environment causes a strong color variation ΔE (more than 11) in the alkali-activated slag-based mortars AAS8 probably due to the high superficial roughness compared to the other mixtures investigated in this research.

The addition of TiO_2 drastically reduces color variations of all the samples exposed to South of about 40–60% compared to the reference mixtures without titanium dioxide. However, the self-cleaning capability is only marginally influenced by the dosage of nanoparticles; in fact, 2-year ΔE of samples made with 1, 3 or 5% of TiO_2 appear very similar with differences not detectable by human eyes, in general lower than 0.5. This limited color variation of samples containing titanium dioxide is clearly ascribable to the photocatalytic activity of TiO_2 and not to a different fouling resistance of the surfaces as confirmed also with the dirt pick-up resistance tests previously reported.

As expected, different exposures modify the efficiency of the titanium dioxide as photocatalyst in mortars due to the lower solar irradiation in the 45°-tilted North-faced surfaces with respect to the South-faced ones. The different exposure to natural light caused significantly distinct color variation of specimens exposed to the industrial environment. It was measured an increased 2-year ΔE up to 3 in the samples with titanium dioxide while no significant differences were detected in reference mortars without nanoparticles (Fig. 13 right).

Finally, from the spectrophotometric measurements a superficial yellowing of the specimens is evident which is expressed through an increase of the color coordinate b* shown in Fig. 14. This color variation evolves quickly in the first weeks of exposure and then stabilizes over time around values that mainly depend on the titanium dioxide content. In fact, as the TiO_2 content increases, yellowing also increases: the increasing of b* is close to 1.5 for mortars with 1% of TiO_2 while is about 2.0 and 2.5 when 3 or 5% of titanium dioxide nanoparticles is used, respectively. However, there is also a slight yellowing of the reference samples without nanoparticles. This behavior is generally related to the surface soiling, degradation of organic admixtures in mortars and mineralization of organic pollutants previously absorbed on the surface [20,39]. Taking into account the limited dosage of superplasticizer in cementitious mixtures, the yellowing of the samples may indirectly indicate that the mortars, in addition to their self-cleaning characteristics, also contribute to the degradation of polluting compounds in the atmosphere.

6. Conclusions

This experimental study was aimed at evaluating the effect of the addition of titanium dioxide nanoparticles on the properties of one-part alkali-activated slag-based mortars in comparison with traditional cementitious mixtures. The following conclusions can be drawn:

- The fresh state properties of mortars are not significantly influenced by the addition of TiO_2 nanoparticles. It can be observed only a reduction in the setting times by increasing the titanium dioxide dosage;
- The TiO_2-doped mortars AAS8 and the reference mixtures based on Portland cement show an enhancement in the compressive strength and elastic modulus with the addition of nanoparticles. On the contrary, only negligible improvements can be noticed on AAS mortars with high activator-to-slag ratios;

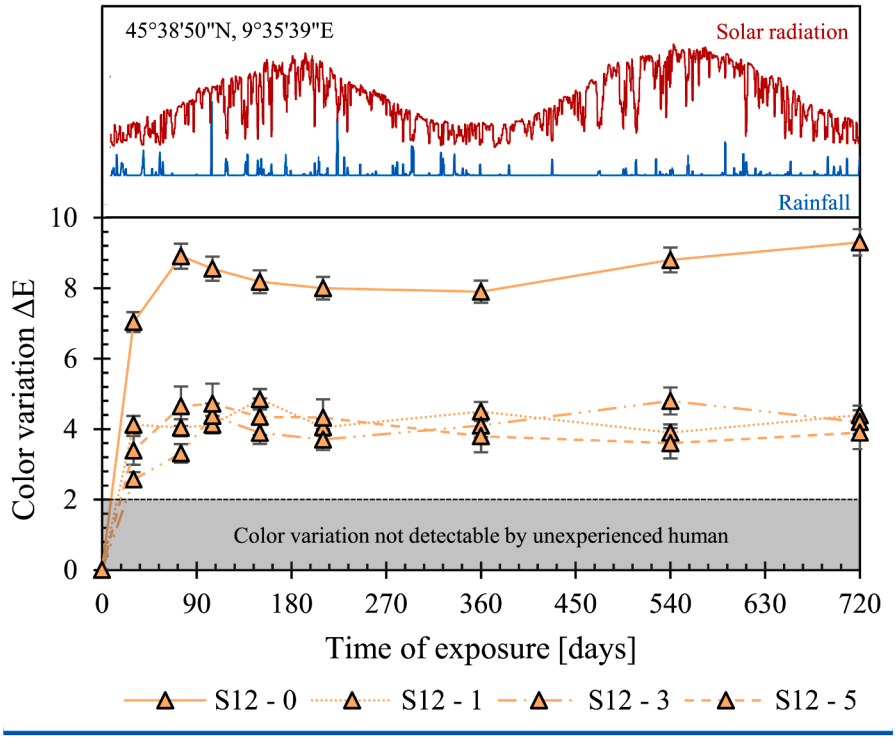

Fig. 12. Top: Rainfall and global radiation during the outdoor exposure (data from Arpa – Regional Agency for Environmental Protection). Bottom: Color variation ΔE as a function of exposure time for S12 mortars with different TiO_2 content (South exposure). The limit of color detection by humans is from [38].

Table 9
Initial color coordinates of samples, CIELab space (L*; a*; b*). The color of the cells represents the color coordinates of samples.

	0%	1%	3%	5%
WC	(80.73;0.58;2.78)	(83.18;0.56;2.40)	(82.41;0.52;2.78)	(81.40;0.22;2.38)
GC	(69.50;-0.27;0.65)	(68.70;-0.34;0.70)	(70.26;-0.25;0.71)	(70.56;-0.23;0.69)
S8	(72.96;1.84;7.28)	(73.37;1.67;7.04)	(76.03;1.37;6.16)	(78.08;1.15;5.84)
S12	(75.49;1.70;7.04)	(76.99;1.52;6.40)	(76.28;1.40;5.95)	(79.51;1.11;5.30)
S16	(78.18;1.36;6.29)	(79.46;1.38;6.30)	(77.72;1.23;5.60)	(79.81;1.20;5.29)

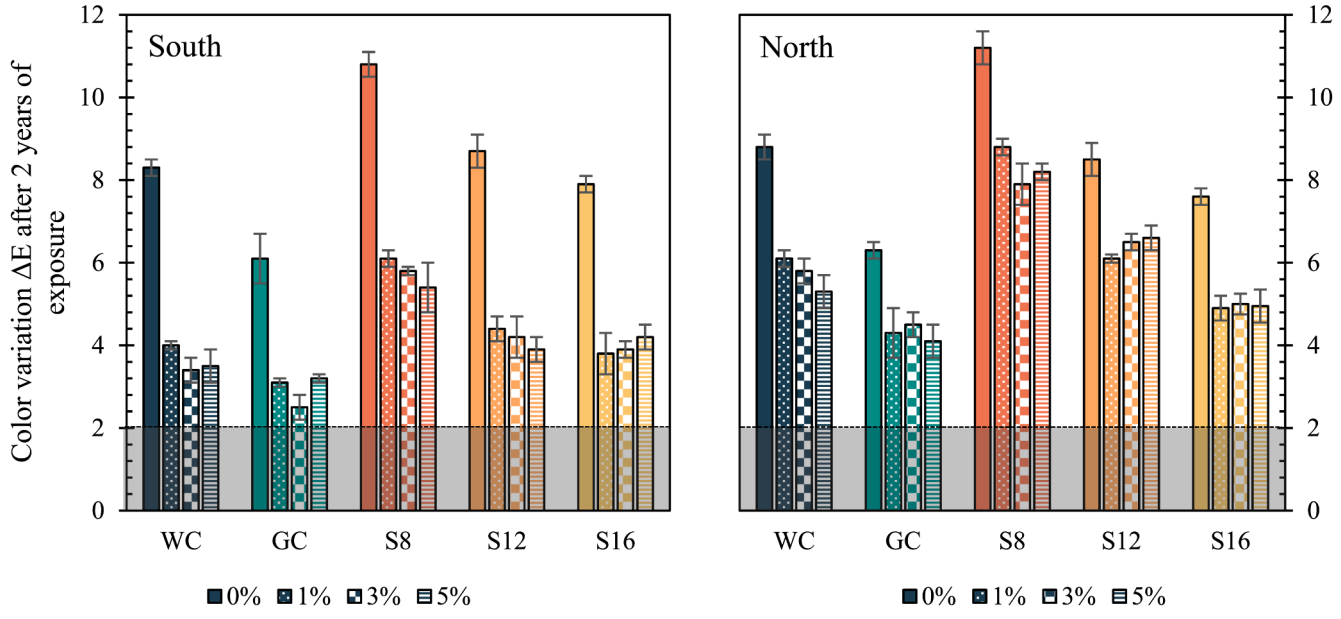

Fig. 13. Color variation of mortars after 2 years of exposure to industrial environment. On the left the South exposure, on the right the North ones. The grey area represents the color variation not detectable by unexperienced human.

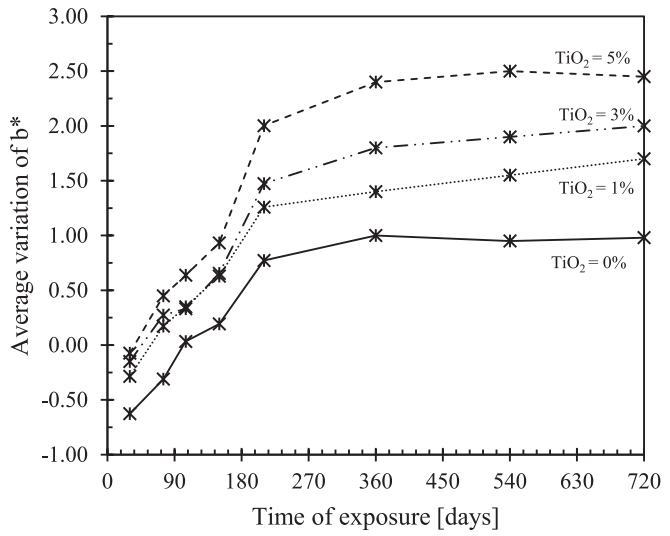

Fig. 14. Variation of b* color coordinate as a function of exposure time for samples containing different amount of titanium dioxide. The average value is calculated on samples manufactured with different binders (cementitious and alkali-activated) exposed to North or South.

- The RhB and MB photodegradation shows a pronounced beneficial effect of TiO_2 addition in self-cleaning capability in both cementitious and alkali-activated mortars. However, alkali content in AAS mortars plays a fundamental role in the photocatalytic efficiency of the titanium dioxide nanoparticles: the higher the alkali content, the higher the efficiency coefficient Γ;
- The dirt pick-up resistance is strongly influenced by the superficial roughness and porosity of mortars but it not depends to the addition of nanoparticles;
- TiO_2 nanoparticles are responsible for a reduction of about 40–60% in color variation after 2 years of exposure in an industrial environment, independently of dosage and binder type. Moreover, the superficial yellowing of samples may indicate that the self-cleaning mortars are also able to degrade the polluting compounds in the environment.

CRediT authorship contribution statement

D. Coffetti: Conceptualization, Investigation, Methodology, Visualization, Writing – original draft, Writing – review & editing. **E. Crotti:** Conceptualization, Investigation, Writing – original draft. **L. Coppola:** Conceptualization, Resources, Supervision, Validation, Writing – review & editing.

Declaration of Competing Interest

The authors declare that they have no known competing financial interests or personal relationships that could have appeared to influence the work reported in this paper.

Data availability

Data will be made available on request.

Acknowledgements

The authors want to thank Dr. Alessandro Carrozza (University of Bergamo) for performing the SEM-EDS measurements.

References

[1] A. Fujishima, K. Honda, Electrochemical photolysis of water at a semiconductor electrode, Nature 238 (1972) 37–38, https://doi.org/10.1038/238037a0.
[2] A. Fujishima, X. Zhang, D.A. Tryk, TiO2 photocatalysis and related surface phenomena, Surf. Sci. Rep. 63 (2008) 515–582, https://doi.org/10.1016/j.surfrep.2008.10.001.
[3] M. Janczarek, Ł. Klapiszewski, P. Jędrzejczak, I. Klapiszewska, A. Ślosarczyk, T. Jesionowski, Progress of functionalized TiO2-based nanomaterials in the construction industry: a comprehensive review, Chem. Eng. J. 430 (2022), 132062, https://doi.org/10.1016/j.cej.2021.132062.
[4] J. Chen, S.C. Kou, C.S. Poon, Hydration and properties of nano-TiO 2 blended cement composites, Cem. Concr. Compos. 34 (2012) 642–649, https://doi.org/10.1016/j.cemconcomp.2012.02.009.
[5] M.V. Diamanti, M. Ormellese, M.P. Pedeferri, Characterization of photocatalytic and superhydrophilic properties of mortars containing titanium dioxide, Cem. Concr. Res. 38 (2008) 1349–1353, https://doi.org/10.1016/j.cemconres.2008.07.003.
[6] A. Folli, C. Pade, T.B. Hansen, T. De Marco, D.E. MacPhee, TiO2 photocatalysis in cementitious systems: Insights into self-cleaning and depollution chemistry, Cem. Concr. Res. 42 (2012) 539–548, https://doi.org/10.1016/j.cemconres.2011.12.001.
[7] B.Y. Lee, A.R. Jayapalan, M.H. Bergin, K.E. Kurtis, Photocatalytic cement exposed to nitrogen oxides: effect of oxidation and binding, Cem. Concr. Res. 60 (2014) 30–36, https://doi.org/10.1016/j.cemconres.2014.03.003.
[8] S.S. Lucas, V.M. Ferreira, J.L.B. de Aguiar, Incorporation of titanium dioxide nanoparticles in mortars — influence of microstructure in the hardened state properties and photocatalytic activity, Cem. Concr. Res. 43 (2013) 112–120, https://doi.org/10.1016/j.cemconres.2012.09.007.
[9] J.K. Sikkema, S.K. Ong, J.E. Alleman, Photocatalytic concrete pavements: Laboratory investigation of NO oxidation rate under varied environmental conditions, Constr. Build. Mater. 100 (2015) 305–314, https://doi.org/10.1016/j.conbuildmat.2015.10.005.
[10] M.M. Hassan, H. Dylla, L.N. Mohammad, T. Rupnow, Evaluation of the durability of titanium dioxide photocatalyst coating for concrete pavement, Constr. Build. Mater. 24 (2010) 1456–1461, https://doi.org/10.1016/j.conbuildmat.2010.01.009.
[11] A. Maury-Ramirez, W. De Muynck, R. Stevens, K. Demeestere, N. De Belie, Titanium dioxide based strategies to prevent algal fouling on cementitious materials, Cem. Concr. Compos. 36 (2013) 93–100, https://doi.org/10.1016/j.cemconcomp.2012.08.030.
[12] A. Strini, S. Cassese, L. Schiavi, Measurement of benzene, toluene, ethylbenzene and o-xylene gas phase photodegradation by titanium dioxide dispersed in cementitious materials using a mixed flow reactor, Appl. Catal. B Environ. 61 (2005) 90–97, https://doi.org/10.1016/j.apcatb.2005.04.009.
[13] A.M. Ramirez, K. Demeestere, N. De Belie, T. Mäntylä, E. Levänen, Titanium dioxide coated cementitious materials for air purifying purposes: Preparation, characterization and toluene removal potential, Build. Environ. 45 (2010) 832–838, https://doi.org/10.1016/j.buildenv.2009.09.003.
[14] J. Chen, C. Poon, Photocatalytic construction and building materials: From fundamentals to applications, Build. Environ. 44 (2009) 1899–1906, https://doi.org/10.1016/j.buildenv.2009.01.002.
[15] A.A. Bawono, Z.H. Tan, A.H. Hamdany, N. NguyenDinh, S. Qian, B. Lechner, E.-H. Yang, Bright and slip-proof engineered cementitious composites with visible light activated photo-catalysis property for pavement in tunnels, Cem. Concr. Compos. 114 (2020), 103788, https://doi.org/10.1016/j.cemconcomp.2020.103788.
[16] V. Francioso, C. Moro, I. Martinez-Lage, M. Velay-Lizancos, Curing temperature: A key factor that changes the effect of TiO2 nanoparticles on mechanical properties, calcium hydroxide formation and pore structure of cement mortars, Cem. Concr. Compos. 104 (2019), 103374, https://doi.org/10.1016/j.cemconcomp.2019.103374.
[17] J. Yuenyongsuwan, S. Sinthupinyo, E.A. O'Rear, T. Pongprayoon, Hydration accelerator and photocatalyst of nanotitanium dioxide synthesized via surfactant-assisted method in cement mortar, Cem. Concr. Compos. 96 (2019) 182–193, https://doi.org/10.1016/j.cemconcomp.2018.11.024.
[18] E. Bahşi, O. Şahin, H. İlcan, B. Uzal, M.F. Günal, G. Yıldırım, M. Şahmaran, Role of inclusion size distribution of titanium dioxide on the nitrogen oxides reduction capability and microstructural characteristics of cementitious systems, Constr. Build. Mater. 318 (2022), 125992, https://doi.org/10.1016/j.conbuildmat.2021.125992.
[19] M.V. Diamanti, R. Paolini, M. Rossini, A.B. Aslan, M. Zinzi, T. Poli, M.P. Pedeferri, Long term self-cleaning and photocatalytic performance of anatase added mortars exposed to the urban environment, Constr. Build. Mater. 96 (2015) 270–278, https://doi.org/10.1016/j.conbuildmat.2015.08.028.
[20] M.V. Diamanti, N. Luongo, S. Massari, S. Lupica Spagnolo, B. Daniotti, M. P. Pedeferri, Durability of self-cleaning cement-based materials, Constr. Build. Mater. 280 (2021) 122442.
[21] T. Luukkonen, Z. Abdollahnejad, J. Yliniemi, P. Kinnunen, M. Illikainen, One-part alkali-activated materials: a review, Cem. Concr. Res. 103 (2018) 21–34, https://doi.org/10.1016/j.cemconres.2017.10.001.
[22] J.L. Provis, A. Palomo, C. Shi, Advances in understanding alkali-activated materials, Cem. Concr. Res. 78 (2015) 110–125, https://doi.org/10.1016/j.cemconres.2015.04.013.

[23] D. Coffetti, E. Crotti, G. Gazzaniga, M. Carrara, T. Pastore, L. Coppola, Pathways towards sustainable concrete, Cem. Concr. Res. 154 (2022), 106718, https://doi.org/10.1016/j.cemconres.2022.106718.
[24] E.A. Llano-Guerrero, L.Y. Gómez-Zamorano, E. Jiménez-Relinque, Effect of the addition of TiO2 nanoparticles in alkali-activated materials, Constr. Build. Mater. 245 (2020), 118370, https://doi.org/10.1016/j.conbuildmat.2020.118370.
[25] I.M. El-Kattan, M.S. Saif, M.O.R. El-Hariri, A.H. Elgandy, L. Pérez-Villarejo, D. Eliche-Quesada, Assessing the individual impact of magnesia and titania nanoparticles on the performance of alkali-activated slag mortars, Constr. Build. Mater. 365 (2023), 130103, https://doi.org/10.1016/j.conbuildmat.2022.130103.
[26] S.-L. Zhang, X.-Q. Qi, S.-Y. Guo, J. Ren, J.-Z. Chen, B. Chi, X.-C. Wang, Effect of a novel hybrid TiO2-graphene composite on enhancing mechanical and durability characteristics of alkali-activated slag mortar, Constr. Build. Mater. 275 (2021), 122154, https://doi.org/10.1016/j.conbuildmat.2020.122154.
[27] L.Y. Yang, Z.J. Jia, Y.M. Zhang, J.G. Dai, Effects of nano-TiO2 on strength, shrinkage and microstructure of alkali activated slag pastes, Cem. Concr. Compos. 57 (2015) 1–7, https://doi.org/10.1016/j.cemconcomp.2014.11.009.
[28] S.-D. Wang, K.L. Scrivener, P.L. Pratt, Factors affecting the strength of alkali-activated slag, Cem. Concr. Res. 24 (6) (1994) 1033–1043.
[29] L. Coppola, D. Coffetti, E. Crotti, S. Candamano, F. Crea, G. Gazzaniga, T. Pastore, The combined use of admixtures for shrinkage reduction in one-part alkali activated slag-based mortars and pastes, Constr. Build. Mater. 248 (2020) 118682.
[30] T. Meng, Y. Yu, X. Qian, S. Zhan, K. Qian, Effect of nano-TiO 2 on the mechanical properties of cement mortar, Constr. Build. Mater. 29 (2012) 241–245, https://doi.org/10.1016/j.conbuildmat.2011.10.047.
[31] M. Suneel, K. Jagadeep, K.K. MahaLakshmi, G. Praveen Babu, G.V. Ramarao, An experimental study on workability and strength characteristics of M40 grade concrete by partial replacement of cement with nano-TiO2, in: B.B. Das, N. Neithalath (Eds.), Sustain. Constr. Build. Mater., Springer Singapore, Singapore, 2019, pp. 253–263.
[32] A. Kashani, J.L. Provis, G.G. Qiao, J.S.J. Van Deventer, The interrelationship between surface chemistry and rheology in alkali activated slag paste, Constr. Build. Mater. 65 (2014) 583–591, https://doi.org/10.1016/j.conbuildmat.2014.04.127.
[33] R. Zhang, X. Cheng, P. Hou, Z. Ye, Influences of nano-TiO2 on the properties of cement-based materials: Hydration and drying shrinkage, Constr. Build. Mater. 81 (2015) 35–41, https://doi.org/10.1016/J.CONBUILDMAT.2015.02.003.
[34] D. Shafaei, S. Yang, L. Berlouis, J. Minto, Multiscale pore structure analysis of nano titanium dioxide cement mortar composite, Mater. Today Commun. 22 (2020), 100779, https://doi.org/10.1016/j.mtcomm.2019.100779.
[35] V.V. Tyukavkina, E.A. Shchelokova, A.V. Tsyryatyeva, A.G. Kasikov, TiO2–SiO2 nanocomposites from technological wastes for self-cleaning cement composition, J. Build. Eng. 44 (2021), 102648, https://doi.org/10.1016/j.jobe.2021.102648.
[36] W. Shen, C. Zhang, Q. Li, W. Zhang, L. Cao, J. Ye, Preparation of titanium dioxide nano particle modified photocatalytic self-cleaning concrete, J. Clean. Prod. 87 (2015) 762–765, https://doi.org/10.1016/j.jclepro.2014.10.014.
[37] Q. Zhu, N. Liu, N. Zhang, Y. Song, M.S. Stanislaus, C. Zhao, Y. Yang, Efficient photocatalytic removal of RhB, MO and MB dyes by optimized Ni/NiO/TiO2 composite thin films under solar light irradiation, J. Environ. Chem. Eng. 6 (2018) 2724–2732, https://doi.org/10.1016/J.JECE.2018.04.017.
[38] W.S. Mokrzycki, M. Tatol, Colour difference ΔE – a survey, Mach. Graph. Vis. 20 (2011) 383–411.
[39] K. Hashimoto, H. Irie, A. Fujishima, TiO 2 photocatalysis: A historical overview and future prospects, Japanese J. Appl. Physics, Part 1 Regul. Pap. Short Notes Rev. Pap. 44 (2005) 8269–8285. doi: 10.1143/JJAP.44.8269.